CHARGE MOBILIZATION BEHAVIOR OF POLYANILINE- A-AMINO ACIDS COMPOSITES

A. Ananda Jebakumar[1]*, P. Sumithraj Premkumar[2] J. Ilavarasi Jeyamalar[3] and C. Ravi Samuel Raj[3]

Article History: Received: 10.04.2023 **Revised:** 15.05.2023 **Accepted:** 30.05.2023

Abstract

Towards exploring charge transfer behavior in polyaniline based composites design and study are alarming. This work is intended to study the charge mobilisation behavior by measuring the DC conductance of four different compositions of PANI-α-amino acids together with DFT, synthesis and physic-chemical studies. The composites are PANI-L-cysteine hydrochloride, PANI-L-serine and ES-L-tyrosine. Computational structural and TDDFT measurements were performed through B3LYP/6-31G** and PBE0/TZV.It was observed that the amino acids retard the charge mobilisation in the PANI and PANI-TYR has higher mechanical strength.

Keywords: PANI, amino acid, DFT, composite, conductance,NLO

[1]Department of Chemistry, Government Polytechnic College for Women, Madurai, Tamilnadu, India-625011
[2]Department of Physics, St. John's College , Palayamkottai, Tirunelveli district, Tamilnadu, India –627002
[3]Department of Chemistry, Pope's College (Autonomous), Sawyerpuram, Thoothukudi district, Tamilnadu, India – 628251

Email: anandajebakumar@gmail.com, psumithraj@gmail.com, ilavarasichem@gmail.com, ravisamuelraj@gmail.com

DOI: 10.31838/ecb/2023.12.si6.132

1. Introduction

Charge transfer phenomenon in the polymer interface is a most exciting physical phenomenon, both as a source of information on materials and also due to its huge scope in nanoelectronics and device applications [1]. Polyaniline (PANI),a conducting polymer has attractive features due to its mechanical flexibility, ease of processing, modifiable electricalproperties and compositing nature [2]. Compositing results with attractive materials through adjusting the chemical and physical properties through the additive [3]. PANI is an intrinsic conducting polymer consisting of phenylenediamine and quinonediimine structure stabilized by resonance structures resembles the aromatic or quinoid forms [4]. In its neutral state PANI is not a conductor and becomes conductor only in the oxidized state [5].The charge associated with the oxidized state is typically delocalized over several units of this polymer and can form a radical cation, polaron or a dication, bipolaron [6]. Compositing of PANI alters its electronic structure as well environment resulting with the modification in the structure, activity besides applications[7].Computational study gives a lot of information about a system of study, which leads to a better understanding and helps to tailor a system. In this scenario DFT method provides accurate information about the electronic environment of the molecule [8]. A good number of works are available for the composites of PANI [9] and DFT [10].

The present investigation focuses on the study mobilisation behavior of PANI through compositing by measuring their electrical conductance along with computational assisted explanations. Here emeraldine salt of PANI and thio base α-amino acids (AA)PANI-L-cysteine hydrochloride (PANI-CYSHC), PANI-L-serine (PANI-SER) and ES-L-tyrosine (PANI-TYR) composites are synthesized, characterised and

physic-chemical properties are studied along with computation.

2. Experimental

2.1 Synthesis of PANI

All the chemicals used were of AR grade obtained from Merk, India and used as such.

10 g of anilineand 30.6 g of ammoniumperdisulphate were dissolved in 1M 250ml HCl separately and cooled them at 18°C. Ammoniumperdisulphate solution was added dropwise to the aniline solution with constant stirring for about 50 minutes. The content was kept aside for 12 hours and washed with water containing a small amount of acetone. Then the content was filtered, dried at 80^{o}C for 8 hours and stored in a polyethylenecontainer. Water was used as a solvent.The yield is 58%. Basic unit weight is 92. The percentage doping of HCl in PANI was measured by titrating a known amount of PANI with standard alkali.

2.2Synthesis of Composites

Slurry was prepared by 400mg of ES and 100 mg of CYSHC4 ml in DMSO for using mortar and pestle. The content was dried at 70 ^{o}C for 24 hrs. Weight loss method was employed to check the complete removal of DMSO from the mixture. The composite was powdered and stored in a polyethylene container. The same procedure was repeatedwith200, 300 and 400 mg of CYSHC and amino acids.

2.3 Computation

DFT studies were pe rformedby B3LYP/6-31G** basis set in the gas phase at 25 °C using firefly software [11] in i7 computer. TDDFT calculations were done using ORCA programme [12] by PBE0/TZV. Due to higher computational cost, the modeling studies were carried for each one unit of phenyl and phenylene rings for PANI.

2.4 Equipment

DC conductance was studied in four probes SES-Model DFP-RM. IR spectra were recorded in JASCO FT/IR-4600, UV-VIS in JASCO V-650 (DMSO Solvent) and Luminescence in Perkin Elmer, LS 45, excitation at 380 nm (DMSO Solvent).

2.5 Analysis

Regression analysis was carried out for conductance studies. The equations used were; for ideal-$y = y_0+ax$; for real- $y = y_0+ax+bx^2$. The ideal behaviour means expected. Pearson's correlation coefficients for ideal and real behaviours were calculated using software SPSS 16 [9].

3. Results and Discussion

The studiedPANI-CYSHC, PANI-SER andPANI-TYR composites the α-amino acids have a hetero group as a side chain. The side chains are thiol, alcohol and phenol respectively for CYSHC, SER and TYR. CYSHC is in the salt form. Computations were performed by attaching the α-amino acid to the N_{14}(Fig. 1), where the steric effect is less and it is not protonated in the PANI.

3.1 Stability and Structure

Fig. 1 has the stability and structure of this group. The stability is directly related to the binding force between the PANI and AA and inversely related to the steric effect caused by the AA on PANI. The stability order is PANI-CYSHC >PANI-SER >PANI-TYR. The bulkier AA causes distortion in the PANI backbone and reduces the overall stability [13]. The relative instability of PANI-SER and PANI-TYR are 26 and 28% with respect to PANI-CYSHC. Here the higher stability PANI-CYSHC may be due to lower steric effect caused by CYSHC, due to higher intra-molecular aggregation [14]. The relative instability of PANI-TYR can be accounted for the higher steric effect caused by the bulky phenyl ring over SH and OH groups. The stability factor partially matches the measured conductance (Table 1). The higher stability of PANI-CYSHC over PANI-SER may be due to the salt form of the former. It is worth to be mention here PANI-TYR composite is harder and this hardness may be due to the increase in the covalent nature of the composite. Further, this property can be justified by low dipole moment(Table3) of PANI-TYR over PANI and their corresponding additive.

The structural data are given in Table 1. Based on the $H_{1'}$-$Cl_{2'}$ and N_1-$H_{1'}$ bond lengths, binding strength between $H_{1'}$ and N_1 is of the order (w.r.t. PANI=100%) PANI-TYR (81%) >PANI-SER(65%) > PANI-CYSHC (59%). As the conductivity, a measure of electron mobilization ability,of PANI is caused by the movement of $H_{1'}$ [15], the weaker binding of $H_{1'}$ with polymer reduces the drift effect and their by retard the conductivity. The difference in the binding order and the experimental conductancecan be accounted for by steric effect as well as excess protonation of PANI by additional HCl in CYSHC.

Except dihedral $Cl_{2'}$-$H_{1'}$-N_1-C_2, otherangleshave no significant change compared to PANI. Based on the above dihedral, the approach angle of $H_{1'}$-$Cl_{2'}$ in PANI-SER is comparable with PANI. Thus, the higher conductance of PANI -SER may be attributed to their lesser reorientation of the electron cloud in the molecule and maintains the approach angle of $H_{1'}$-$Cl_{2'}$ comparable with PANI [16].

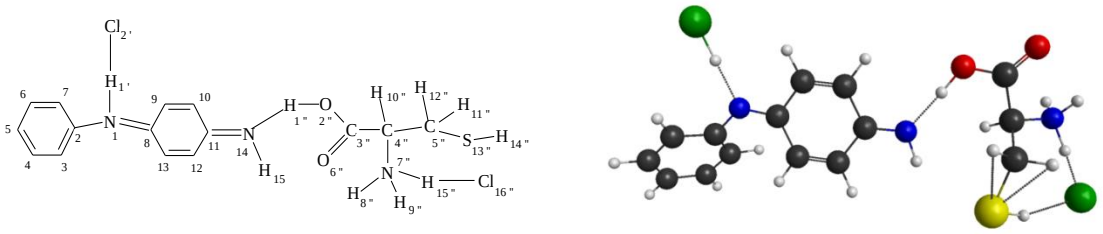

ES-CYSHC

(ES-CYSHC - (ES+CYSHC) = -71.2298 kJ/mole)

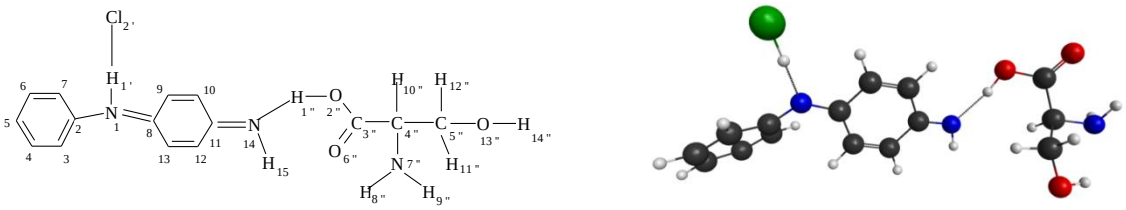

ES-SER

(ES-Serine- (ES+SER) = -52.5625 kJ/mole)

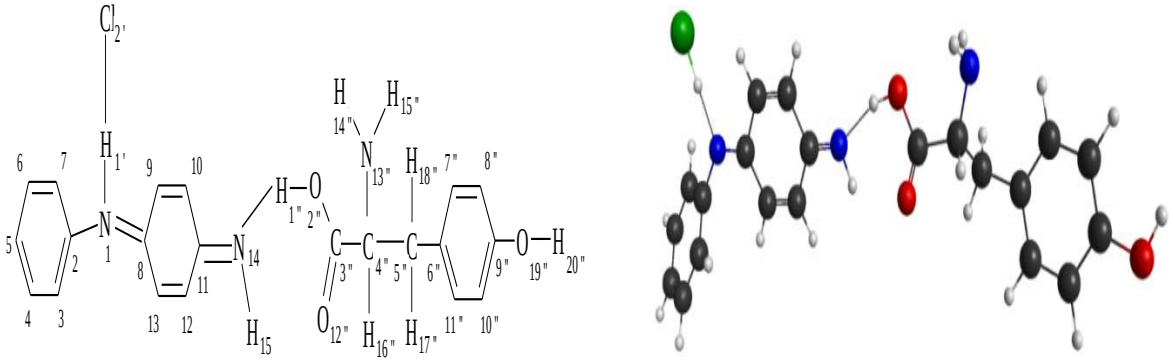

ES-TYR

(ES-TYR- (ES+ TYR) = -51.2497 kJ/mole)

C-Black; H-White; O- Red; N-Blue; Cl-Green; S-Yellow.

Figure 1 : Structure and Thermodynamic Stability

3.2 Charge Density

Table 2 has the Mulliken atomic charge density. Based on the charge density of N_1, $H_{1'}$ and $Cl_{2'}$, it is inferred that the $H_{1'}$-$Cl_{2'}$ binding in the PANI-AA is less intense than PANI. The order of binding is PANI-TYR >PANI-SER >PANI-CYSHC with a ratio of 2:1:0.8. This order is comparable with the previous section and has contradicted the experimental conductance. That is, the expected conductance of PANI -TYR must be greater than that of other PANI-AA, but it is not so. This result can be accounted as the structural effect of PANITYR dominates over the electronic effect [17].

Table 2 : Mulliken's Atomic Charge Density

ES-CYSHC		ES-SER		ES-TYR	
Atom	**Charge**	**Atom**	**Charge**	**Atom**	**Charge**
$H_{1'}$	0.1732	$H_{1'}$	0.1752	$H_{1'}$	0.1811
$Cl_{2'}$	-0.2821	$Cl_{2'}$	-0.2885	$Cl_{2'}$	-0.3063
N_1	-0.5955	N_1	-0.5984	N_1	-0.6077
C_2	0.2487	C_2	0.2476	C_2	0.2491
C_3	-0.0974	C_3	-0.0974	C_3	-0.0978
C_4	-0.0956	C_4	-0.0959	C_4	-0.0959
C_5	-0.0743	C_5	-0.0755	C_5	-0.0764
C_6	-0.0912	C_6	-0.0917	C_6	-0.0920
C_7	-0.0906	C_7	-0.0905	C_7	-0.0918
C_8	0.3291	C_8	0.3308	C_8	0.3357
C_9	-0.0944	C_9	-0.0983	C_9	-0.1024
C_{10}	-0.0936	C_{10}	-0.0936	C_{10}	-0.0661
C_{11}	0.3505	C_{11}	0.3354	C_{11}	0.3143
C_{12}	-0.1114	C_{12}	-0.1070	C_{12}	-0.1076
C_{13}	-0.0891	C_{13}	-0.0896	C_{13}	-0.0944
N_{14}	-0.6745	N_{14}	-0.6283	N_{14}	-0.6169
H_{15}	0.2725	H_{15}	0.2529	H_{15}	0.2765

3.3 Dipole moment

The dipole moment is a measure of charge polarisation in the molecule and the values are given in Table 3. The percentage variation in the total dipole moment with respect to PANI is 28, 44.2 and -45.3 respectively for PANI-CYSHC, PANI-SER and PANI-TYR. The negative sign indicates a lesser value than ES and vice versa. Thus, the higher conductance of PANI and other PANI-AA over PANI-TYR is due to the predominance of the steric effect over the electronic effect of PANI-TYR.

Table 3: Dipole moment (D)

	μ_x	μ_y	μ_z	μ_{Total}
CYSHC	-3.1541	1.7576	3.8775	5.2983
ES-CYSHC	-8.1109	1.3706	1.1481	8.3056
SER	-0.2817	1.6316	1.3420	2.1313
ES-SER	-4.2813	7.9823	2.3401	9.3553
TYR	0.4027	-2.2497	2.0433	3.0656
ES-TYR	-2.3678	2.5599	-0.6669	3.5503

3.4 Molecular Orbital

In general, the MOs of PANI-AA are closely spaced like bands than AA. The MOs of PANI-AA are comparable with PANI over AA. The band thickness is higher for PANI-TYR. Normally the HOMO of PANI-AAis situated on the AA part while the LUMO is on PANI. In other words, HOMO has AA character and LUMO has PANI character. Thus, a charge transfer transition is expected from the HOMO to LUMO through the hoping mechanism. The percentage change in the stability of HOMO with respect to PANI is of the order PANI-SER (1.2) >PANI-CYSHC(-1.5) >PANI-TYR(-13.1). All the LUMO are stabilised and the order of stability with respect to PANI is PANI-CYHC (41.6%) >PANI-SER (17.3%) >PANI-TYR (9.3%).Hence, the above results confirm that PANI-AA with highly stable HOMO and moderately stable LUMO have higher conductance.

3.5 TDDFT

Data related to TDDFT are given in Table 4. The PANI-AA has each one and two transitions in the visible and UV regions respectively. All the transitions of PANI-AA have redshift with respect to PANI.PANI-CYSHC, the peak at 447.8nm is due to the charge transfer transition from the chloride of CYSHC moiety to the nitrogen atom of

the PANI. Another transition at 312.5 nm is the combination of HOMO-10→LUMOand HOMO-9→LUMO for transitions within PANI. For PANI-SER, the peak in the visible region is due to the charge transfer transition from the SER to the nitrogen of PANI. Other two transitions are within the polymer chain.

The same trend is followed for PANI-TYR and the charge transfer is from the benzene ring of TYR. The order of redshift in the visible region and computed optical bandgap based conductance is PANI-CYSHC>PANI-SER>PANI-TYR. The oscillatory strength also follows the above order. As oscillatory strength is a measure of molecular symmetry, the lower conductance of PANI-TYR can be accounted for the loss of symmetry due to the steric effect. Further, the lesser conductance of PANI-CYSHC overPANI-SER may be due to the hampering of the charge carriers by the excess protonation of PANI by HCl of CYSHC.

Table 4 : TDDFT

ES-CYSHC

Wave Length (nm)	Oscillatory Strength	Orbital	% Contribution
447.8	0.3105	95a→99a	78.66
312.5	0.1759	88a→ 99a 89a →99a	36.44 20.62

ES-SER

Wave Length (nm)	Oscillatory Strength	Orbital	% Contribution
442	0.2815	85a→86a	77.29
313.1	0.2175	76a →86a 78a→86a	35.95 22.67
297.6	0.3204	74a→86a 76a →86a	34.40 33.80

ES-TYR

Wave Length (nm)	Oscillatory Strength	Orbital	% Contribution
429.8	0.2809	102a →106a	77.02
306.4	0.2084	96a → 106a	31.54
294.9	0.3495	93a → 106a 96a → 106a	34.20 35.46

3.6 Frontier Molecular Orbital

Values of the above title are given in Table 5. Based on the FMO studies the expected order of conductance is PANI-CYSHC >PANI-SER >PANI-TYR. As mentioned earlier the lower conductance of PANI-TYR is due to the steric effect. The experimental higher conductance of PANI-SER over PANI-CYSHC is due to the presence of HCl in the later. At the outset, conductivity is the outcome of electronic, steric and chemistry of the materials.

3.7 Polarizability

The values of polarizabilities are given in Table 6. The α and γ-values are higher along the *z*-direction, while β along*xz*-plane. Except for TYR other PANI-AA are having a higher self-focusing effect than AA. The order of polarizability is $\gamma > \alpha > \beta$, which is different from PANI. The values of μ, α_{XZ}, β_{ZZZ} and γ_{ZZZZ} are higher for PANI-SER and may account for its higher conductance. Hence, it may be concluded that the charge mobilisation in PANI-SER is along the *xz*-plane. The order of non-linear focusing effect is PANI-SER >PANI-TYR >PANI-CYSHC.

3.8 Spectra

Computed and experimental spectra are comparable with basis set and gas phase corrections. In general, the IR peaks of PANI-AA had a redshift from PANI. This is attributed to the change in the structural parameters due to the formation of PANI-AA from PANI and AA. The contrary the electronic spectra hasa blue shift for PANI-AA from PANI. The experimental optical bandgap based conductance order is PANI-SER >PANI-CSYHC >PANI-TYR. This trend matches the experimental conductance. There is a marginal change in the optical band gap value between PANI-CSYHC and PANI-TYR. For PANI-AA, the intensity of the peak at~780 nm is very low when compared to PANI. This accounts for the lower conductance of PANI-AA over PANI. The spectral studies confirmed the presence of interaction between PANI and AA moiety. The polaron bands are observed in both IR and UV-VIS regions. The

absorption band near 1290 cm^{-1} is for π-electron delocalization induced in the polymer by protonation [18] and $C–N^{+\bullet}$ stretching vibration in the polaron structure [19]. The peak in wavelength band 250–400 nm is due to π→π* transition of the benzenoid unit, peak at 685 nm is due to the polaron→π* transition and peak in wavelength band 820 nm are attributed to the π*→polaron transition [20,21]. Fluorescence spectra of PANI-AA are comparable with PANI but, with lesser intensity. Photoluminescence of PANI-CYSHC, PANI-SER and PANI-TRY are in violet and red regions.

Table 5 : Frontier Molecular Orbital

	eV								Q^{Max}
	Band Gap	**Ionisation potential**	**Electron affinity**	**Electronic chemical potential**	**Chemical hardness**	**Global softness**	**Electrophilic index**	**Absolute Electronegativity**	
CYSHC	6.0	6.7	0.7	-3.7	3.0	0.3	20.6	3.7	1.2
SER	7.2	7.0	-0.2	-3.4	3.6	0.3	20.7	3.4	0.9
TYR	5.9	5.7	-0.2	-2.7	3.0	0.3	11.1	2.7	0.9
ES-CYSHC	2.3	6.4	4.0	-5.2	1.2	0.9	15.8	5.2	4.5
ES-SER	3.2	6.6	3.3	-4.9	1.6	0.6	19.7	4.9	3.1
ES-TYR	2.5	5.6	3.1	-4.4	1.3	0.8	12.0	4.4	3.5

Table 6 : Polarisability (Au)

Axis	**CYSHC**	**SER**	**TYR**	**ES-CYSHC**	**ES-SER**	**ES-TYR**
μ_Z	1.53	0.528	0.804	0.452	0.921	-0.262
α_{XZ}	-9.13	-0.518	-25.0	-3.14	31.7	-26.0
α_{YZ}	-8.57	-4.24	-29.8	1.73	21.0	-64.5
α_{ZZ}	67.0	40.6	105	127	125	168
β_{XZZ}	-15.8	-8.54	86.3	64.3	52.6	53.8
β_{YZZ}	-5.89	12.9	-11.6	32.6	-1.59	9.38
β_{ZZZ}	10.1	-38.0	-72.6	-8.07	-28.4	-18.9
γ_{ZZZZ}	2750	2610	5560	3570	5100	4160

3.9 Conductance

The conductance values and diagrams are given in Table 7. The bold line in the graph represents the real and dotted line represents the ideal conductance. It was not possible to make pellets for PANI-TYR at higher concentrations of TYR. The conductance is studied using second order algebraic equation. It has two coefficients 'a' and 'b'. Variable 'x' gives the maximum deviation of real conductance from the ideal. Coefficients 'a' and 'b' are to measure the deviating and restoring effects of the ideal behaviour. The order of 'a' and 'b' is PANI-TYR>PANI-CYSHC >PANI-SER. The order may be accounted for by the steric effect.

The mole fraction of PANI at which the highest divergence from optimal behaviour occurs is 0.7032, 0.5526, and 0.8134 for PANI-CYSHC, PANI-SER, and PANI-TYR, respectively. The order of conductance is PANI-SER >PANI-CYSHC >PANI-TYR. The order can be explained as; the higher conductance in PANI-SER is due to less steric effect and higher electronic effect due to the presence of bulky and diffusive sulphur [22,23]. PANI-CYSHC blocks the charge carriers through excess protonation of the polymer chain. In the case of PANI-TYR, the TYR retard the conductance of PANI effectively by interrupting the inter-chain and intra-chain diffusion of charge carriers [24].

The 'y_o' measures the electron delocalizing power of AA and the order is TYR > SER > CYHC. That is the electron delocalised power of the AA are not significantly contribute to the conductance of PANI-AA. Further, the delocalised AA may retard the conductivity of PANI-AA through their effective inter and intra-molecular interactions by blocking the mobility of the charge carriers. Thus, the conductance of PANI-AA depends on the structural effect induced electronic effect and the presence of additional ion. For all the PANI-AA the conductance decreases with an increase of the mole fraction of AA.

Table 7: Conductance

ES-CYSHC

Mole Fraction of ES	Conductance S/cm
1	0.491
0.8498	0.0201
0.7389	0.0051
0.6536	0.0041
0.5859	0.0048

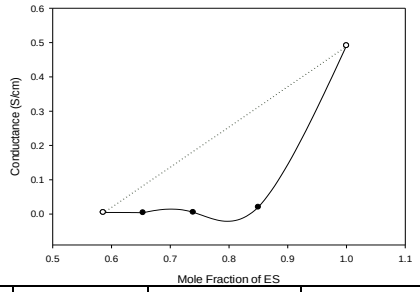

	R	y_0	a	b
Ideal	1.0	-0.68	1.17	-
Real	0.98	2.85	-8.24	5.86

ES-SER

Mole Fraction of ES	Conductance S/cm
1	0.491
0.7905	0.1312
0.6536	0.0652
0.5571	0.0302
0.4854	0.0212

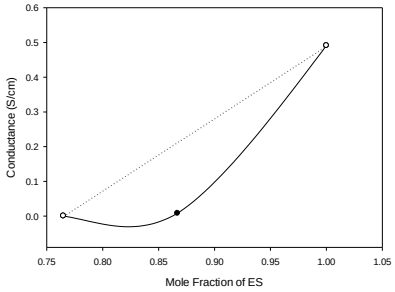

	R	y_0	a	b
Ideal	1.0	-0.42	0.91	-
Real	0.99	0.73	-2.56	2.32

ES-TYR

Mole Fraction of ES	Conductance S/cm
1.0	0.4910
0.8668	0.0080
0.7649	0.0004

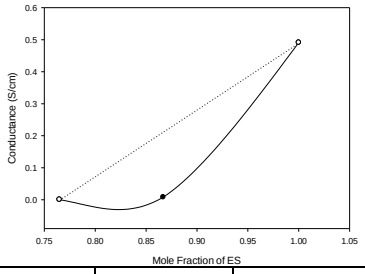

	R	y_0	a	b
Ideal	1.0	-1.60	2.09	-
Real	1.0	9.96	-24.57	15.11

ES-EDTA

Mole Fraction of ES	Conductance S/cm
1	0.491
0.9304	0.0161
0.9176	0.0049
0.9052	0.00172
0.8931	0.00142

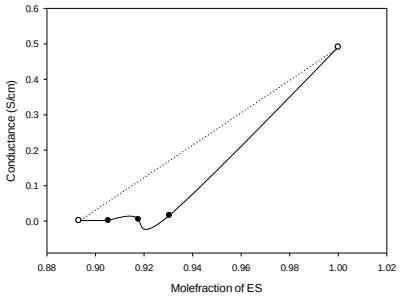

	R	y_0	a	b
Ideal	0.99	-4.088	4.579	-
Real	0.99	48.343	-106.496	58.643

4. Conclusion

This work focuses on the charge mobilisation in the PANI-AA composites of varied proportions through the measurement of DC conductance as well as DFT method. It was observed that PANI-AA composites have lower conductance than PANI due to the dominance of the steric effect over the electronic effect of the composites. Further, the AA disrupts the quantum field of PANI in PANI-AA. The PANI-TYR composite is harder.

References

1. Huilin Wang, Xitong Liang, Jiutian Wang, Shengjian Jiao and Dongfeng Xue, Multifunctional inorganic nanomaterials for energy applications. Nanoscale. 2020;12:14-42.
2. Gagan Kaur, Raju Adhikari, Peter Cass, Mark Bown and Pathiraja Gunatillake, Electrically conductive polymers and composites for biomedical applications. RSC Adv. 2015; 5: 37553-37567.
3. Selvaraj DK, Silva FJG, Campilho RDSG, Baptista A, Pinto GFL, Influence of the natural additive on natural fiber reinforced thermoplastic composite. Procedia Manuf. 2019; 38: 1121–1129.
4. Xin-Gui Li, Mei-Rong Huang, Wei Duan, and Yu-Liang Yang, Novel Multifunctional Polymers from Aromatic Diamines by Oxidative Polymerizations. Chem. Rev. 2002; 102(9): 2925–3030.
5. Mahnoush Beygisangchin, Suraya Abdul Rashid, Suhaidi Shafie, Amir Reza Sadrolhosseini, and Hong Ngee Lim, Preparations, Properties, and Applications of Polyaniline and Polyaniline Thin Films—A Review. Polymers (Basel). 2021; 13(12): 2003.
6. Jin Bakalis, Andrew R. Cook, Sadayuki Asaoka, Michael Forster, Ulrich Scherf, and John R. Miller, Polarons, Compressed Polarons, and Bipolarons in Conjugated Polymers. J. Phys. Chem. 2014; 118(1): 114–125.
7. Jesús Barrio, Michael Volokh and MennyShalom, Polymeric carbon nitrides and related metal-free materials for energy and environmental applications. J. Mater. Chem. A. 2020; 8: 1075-11116
8. Ryo Nagai, Ryosuke Akashi and Osamu Sugino, Completing density functional theory by machine learning hidden messages from molecules. Npj Comput. Mater. 2020; 6: 43.
9. Theresa Sperger, Italo A Sanhueza, and Franziska Schoenebeck, Computation and Experiment: A Powerful Combination to Understand and Predict Reactivities. Acc. Chem. Res. 2016; 49(6): 1311–1319.
10. Giuseppe Felice Mangiatordi, Eric Brémond, and Carlo Adamo, DFT and Proton Transfer Reactions: A Benchmark Study on Structure and Kinetics. J. Chem. Theory Comput. 2012, 8, 9, 3082–3088.
11. Schmidt MW, Baldridge KK, Boatz JA, Elbert ST, Gordon MS, Jensen JH, Koseki S, Matsunaga N, Nguyen KA, Su SJ, Windus TL, Dupuis M & Montgomery JA, General Atomic and Molecular Electronic Structure System. J. Comput. Chem.1993; 14(11), 1347-1363.
12. Frank Neese, The ORCA program system. Wiley Interdiscip. Rev. Comput. Mol. Sci. 2012; 2(1): 73-78.
13. Yue J, Wang ZH, Cromack KR, Epstein AJ, and MacDiarmid AG, Effect of Sulfonic Acid Group on Polyaniline Backbone. J. Am. Chem. Soc. 1991; 113(7): 2665-2671.
14. Vijay Kumar Thakur (eds.), Cellulose-based graft copolymers. Structure and chemistry. 2015; CRC Press, London.
15. Meftah AM, Gharibshahi E, Soltani N, Yunus WMM and Saion E, Structural, Optical and Electrical Properties of PVA/PANI/Nickel Nanocomposites Synthesized by Gamma Radiolytic Method. Polymers. 2014; 6(9): 2435-2450.
16. Yang Zhang, Munan Qiu, Ying Yu, Bianying Wen, and Lele Cheng, A Novel Polyaniline-Coated Bagasse Fiber Composite with Core–Shell Heterostructure Provides Effective Electromagnetic Shielding Performance. Appl. Mater. Interfaces. 2017; 9(1): 809-818.
17. Chen XP, Liang QH, Jiang JK, Cell KY Wong, Stanley Y Y Leung , Ye HY, Yang DG and Ren TL, Functionalization-induced changes in the structural and physical properties of amorphous polyaniline: a first-principles and molecular dynamics study. Sci. Rep. 2016; 6: 20621.
18. Ping Z, In situ FTIR-attenuated total reflection spectroscopic investigations on the base–acid transitions of polyaniline. Base–acid transition in the emeraldine form of polyaniline. J. Chem. Soc., Faraday trans. 1996; 92(17): 3063–3067.
19. Boyer ML, Quillard S, Louarn G, Froyer G and Lefrant S, Vibrational Study of the FeCl3-Doped Dimer of Polyaniline; A Good Model Compound of Emeraldine

Salt, J. Phys. Chem. B. 2000; 104(38): 8952-8961.

20. Francisco J. Melendez, María Eugenia Castro, Oscar Portillo-Moreno, Guadalupe Hernández-Téllez, Gloria E. Moreno-Morale, Daniela Gutiérrez-Argüelles , Rodolfo Palomino-Merino, Efraín Rubio-Rosas and René Gutiérrez-Pérez, Experimental and DFT Study of the Photoluminescent Green Emission Band of Halogenated (−F, −Cl, and −Br) Imines. Molecules. 2019; 24: 3304.
21. Deshpandea NG, Gudage YG, Sharma R, Vyas JC, Kim JB and Lee YP, Studies on tin oxide-intercalated polyaniline nanocomposite for ammonia gas sensing applications. Sens. Actuators B Chem. 2009;138(1): 76-84.
22. Anastasiia N. Andriianova, Yuliya N. Biglova, and Akhat G. Mustafin, Effect of structural factors on the physicochemical properties of functionalized polyanilines. RSC Adv. 2020;10(13): 7468–7491.
23. Anna Parshina, Anastasia Yelnikova, Tatyana Titova, Tatyana Kolganova, Polina Yurova, Irina Stenina, Olga Bobreshova, and Andrey Yaroslavtsev, Multisensory Systems Based on Perfluorosulfonic Acid Membranes Modified with Polyaniline and PEDOT for Multicomponent Analysis of Sulfacetamide Pharmaceuticals. Polymers (Basel). 2022; 14(13): 2545.
24. Victor I. Krinichnyi, VI Multi frequency EPR spectroscopy of conjugated polymers and their nanocomposites. 2017;CRC Press: London.